Eigenvalues," *J. Math Physics*, 38, 104 (1959).
Kevorkian, A. K., and J. Snoek, "Decomposition of Large Scale Systems, Theory and Applications in Solving Large Sets of Non-linear Simultaneous Equations," in *Decomposition of Large Scale Problems*, D. M. Himmelblau, ed., North-Holland/American Elsevier, Amsterdam (1973).
Ledet, W. D., and D. M. Himmelblau, "Decomposition Procedures for Solving Large Scale Systems," in *Advances in Chemical Engineering*, Vol. 8, Academic Press, New York (1970).
Lee, W., J. H. Christensen, and D. F. Rudd, "Design Variable Selection to Simplify Process Calculations," *AIChE J.*, **12**, No. 6, 1104 (1966).
Mah, R. S. H., "Structural Decomposition in Chemical Engineering Computation," paper presented at AIChE 72nd National Meeting, St. Louis, Mo. (1972).
Napthali, L. M., and D. P. Sandholm, "Multicomponent Separation Calculations by Linearization," *AIChE J.*, **17**, No. 1, 148 (1971).
Ramirez, W. F., and C. R. Vesthal, "Algorithms for Structuring Design Calculations," *Chem. Eng. Sci.*, **27**, 2243 (1972).
Soylemez, S., and W. D. Seider, "A New Technique for Precedence Ordering Chemical Process Equation Sets," *AIChE J.*, **19**, 934 (1973).
Stadtherr, M. A., W. A. Gifford, and L. E. Scriven, "Efficient Solution of Design Equations," *Chem. Eng. Sci.*, **29**, 1025 (1974).
Steward, D. V., "On an Approach to Techniques for the Analysis of the Structure of Large Systems of Equations," *SIAM Review*, 4, No. 4, 321 (1962).
———, "Partitioning and Tearing Systems of Equations," *J. SIAM Numer, Anal. Ser. B.*, **2**, No. 2, 345 (1965).
Westerberg, A. W., and F. C. Edie, "Computer Aided Design, Part 1: Enhancing Convergence Properties by the Choice of Output Variable Assignments in the Solution of Sparse Equation Sets," *Chem. Eng. J.*, **2**, 9 (1971*a*).
———, "Computer Aided Design, Part 2: An Approach to Convergence and Tearing in the Solution of Sparse Equation Sets," *ibid.*, 17 (1971*b*).

Manuscript received September 26, 1975; revision received February 12, and accepted February 13, 1976.

The Static Electrification of Particles in Gas-Solids Pipe Flow

HIROAKI MASUDA
TAKAHIRO KOMATSU
and
KOICHI IINOYA

Kyoto University
Kyoto, Japan

Electrostatic characteristics in gas-solids flow in a metal pipe are studied both theoretically and experimentally with particular attention to the collision between particles and pipe wall. Effects of gas velocity and particle diameter on the electrification are also examined.

SCOPE

Static electrification of particles takes place in various kinds of powder handling processes. The charge on particles affect the electrostatic and hydrodynamic behavior of particles. During gas-solids pipe flow, particles are charged through their collisions with the pipe wall (Cole et al., 1969). The charge is usually small, and the force generated by the charge is always directed to the wall. When the pipe is long, the charge affects the radial concentration profile of dust in the pipe as well as particle deposition on the wall (Ström, 1972). Neutralization of charge at the pipe inlet does not suffice to eliminate the charge effect because electrification occurs in the pipe. Electrification may also cause dust explosions. Thus it is important to predict the charge on particles.

Difficulty in evaluating this charge arises from the fact that electrostatic and hydrodynamic effects take place simultaneously. Electrostatic effects are usually smaller than the hydrodynamic ones in short pipes, and direct measurement of the charge on a particle in the test section is extremely difficult.

Under these circumstances, the theoretical estimate of the charge is desirable. There is little previous work on such electrification; the study by Cole et al. (1969) is probably the most relevant.

In the present work, the collisions of particles with the wall were studied experimentally, and several collisional parameters, such as the number of collisions per unit area and unit time, and the area of contact have been obtained. In addition, steel pipes held between two vinyl chloride flanges were inserted in a pneumatic conveyor line, and the currents generated on the pipes were measured for several kinds of powder. From these data a relationship between the experimentally obtained collision characteristics and the electrification of particles was inferred. The effects of air velocity and particle diameter on electrification are presented.

CONCLUSIONS AND SIGNIFICANCE

The static electrification of a dilute suspension of fine solid particles in a flowing gas is due to contact electrification caused by collisions between particles and the pipe wall. The theory developed by Cole et al. (1969) has been modified in light of the experimental results. The collision characteristics such as contact area, number of collisions per unit time and unit area, and duration of contact were examined by photomicrographs of scars caused by the impact of particles on a plastic film covering the inside wall of test section. It is shown that theoretical contact area varies with the type of collision (elastic or inelastic).

The currents generated on the wall were measured for flour, vinyl chloride powder, glass beads, eight grades of quartz sand with particle diameter ranging from 14 to 330 μm, and eight grades of morundum particles ranging from 50 to 760μm. From the results, it was found that the current was approximately proportional to the mean air velocity to the power 1.4 when the contact seemed to be elastic and to the power 1.9 when the contact was inelastic. The experimental results reveal that contact is generally inelastic. It was also found that the current was inversely proportional to the mean particle diameter.

These experiments covered mean air velocities in the range 10 to 30 m/s and mean particle diameters between 10 and 1 000μm.

THEORETICAL BACKGROUND

The electrification of particles may be brought about by charge transfer driven by effective contact potential (Cole et al., 1969). The mechanism of the charge transfer when metals or semiconductors are placed in contact has been explained (Shaw, 1962; Vick, 1953). On the other hand, the contact between two materials when one is an insulator has not yet been adequately explained. However, if only slight impurity is introduced in the insulator, it becomes a semiconductor and can be charged. This also applies when the impurity is confined to the surface of the insulator. Particles are usually more or less contaminated, and particles suspended in a flowing gas are generally semiconductors, in this sense, and can be charged.

At the moment of collision, deformation of the particle or the wall is expected. Charge transfer between the materials proceeds in the very short time of collision. Subsequently, the particle and the wall are rapidly separated, leaving the charges on their surfaces. The state of contact is represented by a parallel plate condenser with a gap of a few Angstrom units (Krupp, 1967) or by the contact transition region (Sze, 1969). In each case, contact may be modeled by an electric circuit containing an electric cell, an internal resistance, and a parallel plate condenser. The condenser is charged to the contact potential difference V_c. The relaxation time τ of the charging is the product of the internal resistance R and the capacitance C. Contact ceases after a time Δt, and charging is brought to an end. Particles are charged and create an electric field. The field force causes leakage of charges from the particles to the wall. The charge of a particle is further reduced by the image charge in the wall. Following the development by Cole et al. (1969), its charge on unit mass of particles is given by

$$\frac{q}{m_p} = \left(\frac{q}{m_p}\right)_o \exp\left\{-\frac{n(x)}{n_o}\right\} + \left(\frac{q}{m_p}\right)_\infty \left[1 - \exp\left\{-\frac{n(x)}{n_o}\right\}\right] \quad (1)$$

At an effective flow length x, a pipe of length of Δx generates an electric current, the sign being opposite to that of the charges on the particles. From Equation (1) its absolute value is given by

$$|I_m| = W \left| \left(\frac{q}{m_p}\right)_\infty - \left(\frac{q}{m_p}\right)_o \right| \exp\left\{-\frac{n(x)}{n_o}\right\}\left[1 - \exp\left\{-\frac{n(\Delta x)}{n_o}\right\}\right] \quad (2)$$

where $(q/m_p)_o$ is the initial charge per unit mass of particles, and n_o, the relaxation number, is given by

$$n_o = \frac{\pi D_p^2/2S}{\left(1 + \frac{3}{4} m \frac{\rho_a D u}{\rho_p D_p \bar{v}}\right)(1 - e^{-\Delta t/\tau})} \quad (3)$$

The maximum possible charge is

$$\left(\frac{q}{m_p}\right)_\infty = \frac{3\epsilon_o V_c/\rho_p D_p z_o}{1 + \frac{3}{4} m \frac{\rho_a D u}{\rho_p D_p \bar{v}}} \quad (4)$$

In the discussion section, it will be shown that $(q/m_p)_o << (q/m_p)_\infty$ and $n(x) << n_o$, $n(\Delta x) << n_o$. Therefore, Equation (2) simplifies to

$$|I_m| \cong W \left| \left(\frac{q}{m_p}\right)_\infty \right| \frac{n(\Delta x)}{n_o} \quad (5)$$

Finally, substitution of Equations (3) and (4) into Equation (5) with $\tau >> \Delta t$ gives

$$|I_m| \cong \frac{W\epsilon_o |V_c| \Delta x \Delta t S}{m_p z_o \tau} \cdot \frac{\Delta n}{\Delta x} \quad (6)$$

In this equation, $\Delta n/\Delta x$ must be evaluated at x.

The relaxation time τ and duration of contact Δt appearing in Equation (3) were not introduced in the previous work (Cole et al., 1969). However, the factor $(1 - e^{-\Delta t/\tau})$ will greatly alter the relaxation number n_o. As a consequence, a particle would require many more collisions than shown by Cole's theory. This result is supported by the experimental work of Masuda et al. (1974). Neither the contact area S nor the number of collisions of a particle per unit length of the pipe, Δn, have previously been measured. These problems will be dealt with in the following sections.

EXPERIMENTAL APPARATUS AND PROCEDURES

In this experiment, a pneumatic conveyor line is operated under suction (Figure 1). A 5 cm steel section 15 cm long is used as the measuring element in the conveyor line. Both ends of this section are insulated with vinyl chloride flanges. The current generated is measured by a galvanometer to which a 2 000 μF condenser is connected in parallel in order to suppress fluctuations. The conveyor lines before and after the test section are grounded at one point. The currents are measured at

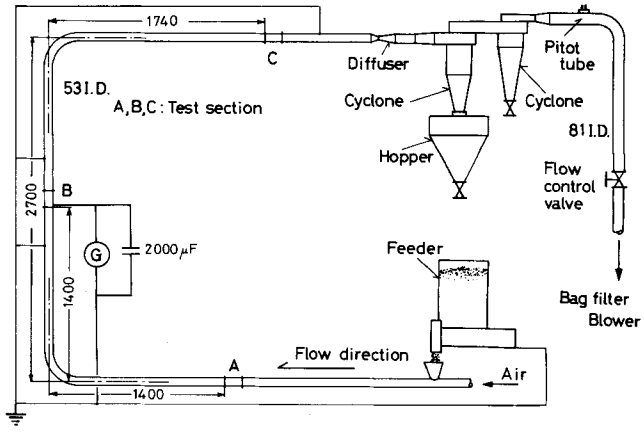

Fig. 1. Experimental setup. (Lengths are shown in millimeters. Test sections A, B, and C are insulated. A, C: horizontal, B: vertical).

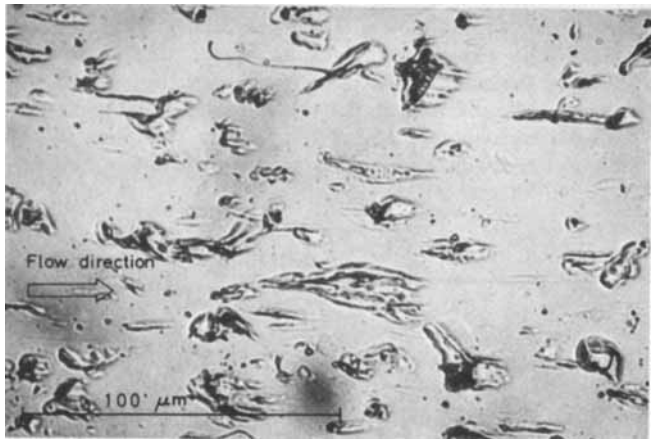

Fig. 2. Photomicrograph of scars on the film wall by particles.

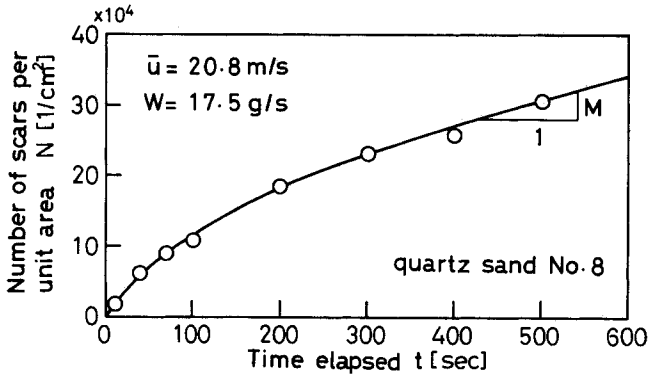

Fig. 3. Number of scars per unit area as a function of time elapsed (position A).

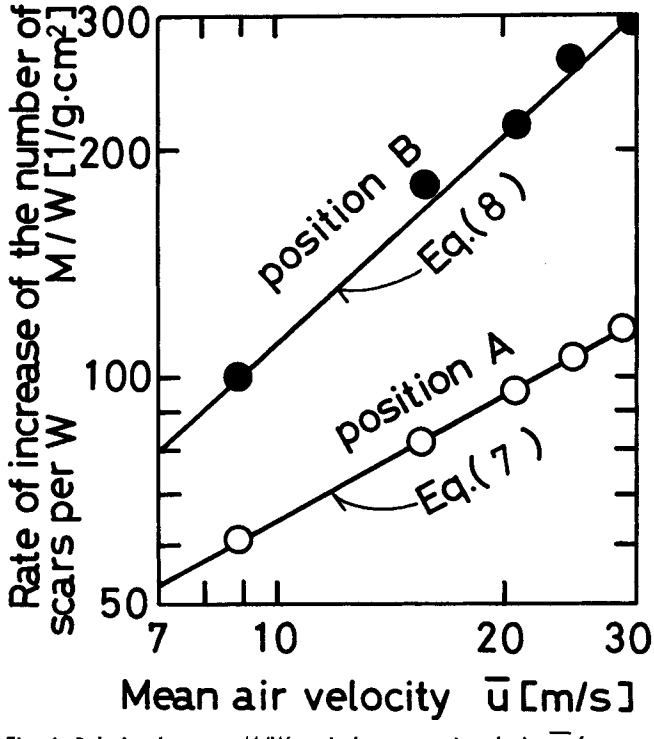

Fig. 4. Relation between M/W and the mean air velocity $\bar{u}$ (quartz sand No. 8).

three positions A, B (vertical), and C shown in Figure 1. These positions are selected to avoid flow disturbance caused by the pipe line inlet and the bends (Masuda et al., 1974). Experimental analysis of the collisions between the particles and the wall covered with a plastic film is also carried out. The plastic film is scratched by bouncing particles, and the scars

TABLE 1. PROPERTIES OF POWDER MATERIALS

Materials	Mass median diam. D_{p50} [μm]	Mean particle diam.* $\overline{D_p}$ [μm]	Density ρ_p[g/cm³]
Quartz sand			
Ultra fine (1)	16.8	14	2.65
No. 8 (2)	51	48	2.65
No. 5 (3)	440	329	2.65
(4)	42	42	2.65
(5)	62	62	2.65
(6)	82	82	2.65
(7)	94	94	2.65
(8)	315	153	2.65
Morundum			
(1)	58	50	3.99
(2)	73	63	3.99
(3)	93	93	3.99
(4)	126	126	3.99
(5)	180	180	3.99
(6)	340	340	3.99
(7)	515	515	3.99
(8)	760	760	3.99
Flour	57	37	1.44
Vinyl chloride	115	111	1.41

* See Equation (22).

are examined by photomicrographs. The photographic results were used to analyze the characteristics of the currents generated on the metal wall. Since the inertia of a particle is very large (inertia parameter: $\rho_p D_p^2 \bar{u}/18\mu D = 4 \sim 12$) and the charge increment of a particle colliding with the plastic film lining test section is very small (smaller than 4×10^{-8} C/g), the collision frequency is unlikely to be affected by the charge due to the short plastic section.

Powder flow rates were measured by a direct weighing method. A calibrated diffuser and a Pitot tube were used to measure the air flow rate. Powders used in the experiments are listed in Table 1.

NUMBER OF COLLISIONS

Figure 2 shows an example of the photomicrographs of the scars made by the impact of quartz sand on the plastic film covering the inside wall. The number of scars per unit area, obtained by counting, is found to be directly proportional to the powder mass flow rate W. The increase of the number from the beginning of powder feeding is shown in Figure 3. After 200 s, the rate of increase is almost independent of the time, showing a stationary value M. The value of the ratio M/W is plotted vs. air velocity in Figure 4 and represented by the following equations:

$$M = 18\,\bar{u}^{0.54}W \qquad \text{at position A} \qquad (7)$$

$$M = 13\,\bar{u}^{0.93}W \qquad \text{at position B} \qquad (8)$$

The units of M, $\bar{u}$, and W are taken in [1/cm² · s], [m/s], and [g/s], respectively. From the material balance of the particles, the average number of collisions of a particle as it passes through unit pipe length $\Delta n/\Delta x$ in Equation (6) is

$$\Delta n/\Delta x = m_p \pi D M/W = \begin{cases} 18\, m_p \pi D \bar{u}^{0.54} & \text{at position A} \\ 13\, m_p \pi D \bar{u}^{0.93} & \text{at position B} \end{cases} \qquad (9)$$

The possible causes of the difference between the M values obtained at positions A and B may be due to the effect of gravity (relative settling velocity: $D_p^2 \rho_p g/18\mu u^* = 0.3 \sim 0.8$) and/or the development of a radial concentration profile of dust along the pipe due in part to the slight electrification of particles.

AREA OF CONTACT

The dimensions of the scars are independent of the powder flow rate but dependent on the mean air velocity. The scar size distribution seems to have its origin in the particle size distribution. The mean widths $\bar{b}$ of the scars are represented by the following relationship as shown in Figure 5:

$$\bar{b} = 1.2\,\bar{u}^{0.53} \tag{10}$$

where the unit of $\bar{b}$ is taken in micrometers. The area of contact $\bar{S}$ can be approximated by the square of the width and is nearly proportional to the mean air velocity.

The collision may be analyzed theoretically to some extent, assuming that each particle is spherical with diameter D_p. Figure 6 shows the conditions at the moment of impact. The normal impulse F_R and the work W_R done by the impulse are obtained by using the equation of particle motion, which is derived from the impulse momentum relations:

$$F_R = -(1+e)m_p v_{ro} \tag{11}$$

and

$$W_R = \frac{1}{2} m_p v_{ro}^2 (1 - e^2) \tag{12}$$

If the incident angle is held constant, these equations with an additional proportional constant are also applicable for a nonspherical particle (Powell and Quince, 1972). In the case of an elastic collision, from Hertz's theory (Timoshenko, 1930), the contact area is given by

$$S = 0.77\,\pi \left(\frac{-F_R}{2\Delta T} \frac{D_p}{E} \right)^{2/3} \tag{13}$$

where the modulus E is represented by the following equation with Young's moduli E_1 for the particle and E_2 for the wall:

$$\frac{1}{E} = \frac{1}{E_1} + \frac{1}{E_2} \tag{14}$$

By substituting Equation (11) into Equation (13), the following equation is obtained:

$$S = 0.77\pi^{5/3} \left\{ \frac{\rho_p (1+e)}{12\,E} \right\}^{2/3} D_p^{8/3} \left(\frac{v_{ro}}{\Delta T} \right)^{2/3} \tag{15}$$

If inelastic deformation occurs during the impact, $W_R = PV$ (Powell and Quince, 1972), where P denotes the constant yield pressure, and V is the deformed volume given by

$$V = \int_{\frac{D_p}{2}-d}^{\frac{D_p}{2}} \pi \left(\frac{D_p^2}{4} - x^2 \right) dx \cong \frac{\pi}{2} D_p d^2 \tag{16}$$

d being the depth. The contact area S is

$$S = \pi \left\{ \left(\frac{D_p}{2} \right)^2 - \left(\frac{D_p}{2} - d \right)^2 \right\} \cong \pi D_p d = \pi \sqrt{\frac{\rho_p (1 - e^2)}{6\,P}}\, D_p^2\, v_{ro} \tag{17}$$

which can be derived from Equations (12), (16), and the relation $W_R = PV$.

From the above analysis, it is found that the area S is proportional to $(v_{ro}/\Delta T)^{2/3}$ for elastic deformation but to v_{ro} for inelastic.* The experimental area of contact is approximately proportional to the mean air velocity as already mentioned in this section. This fact suggests that the deformation is inelastic when quartz sand hits a soft plastic wall, as would be intuitively expected.

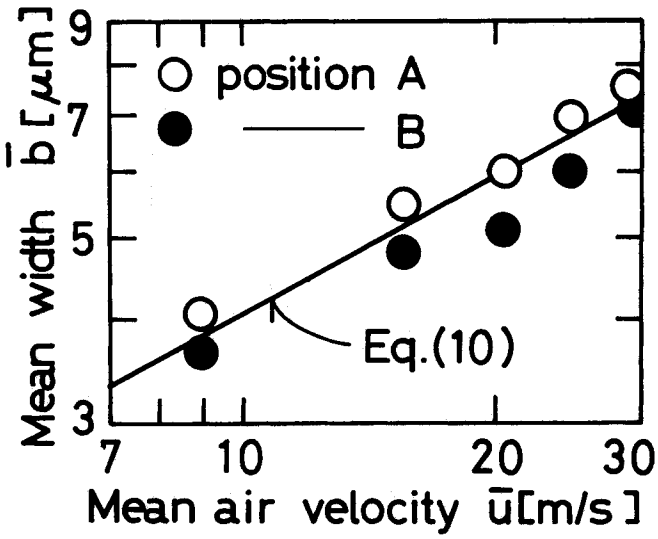

Fig. 5. Mean width of scars (quartz sand No. 8).

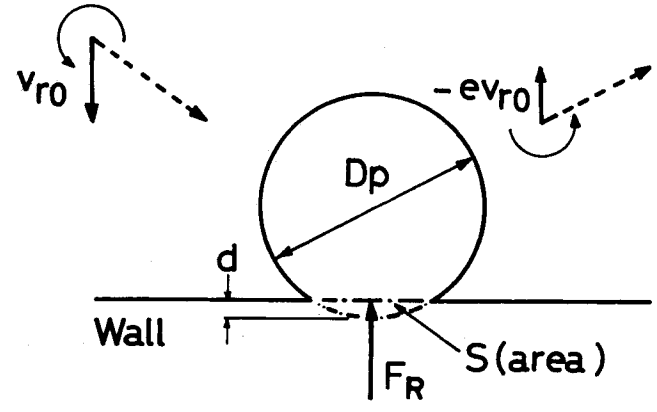

Fig. 6. Impact between a spherical particle and a wall.

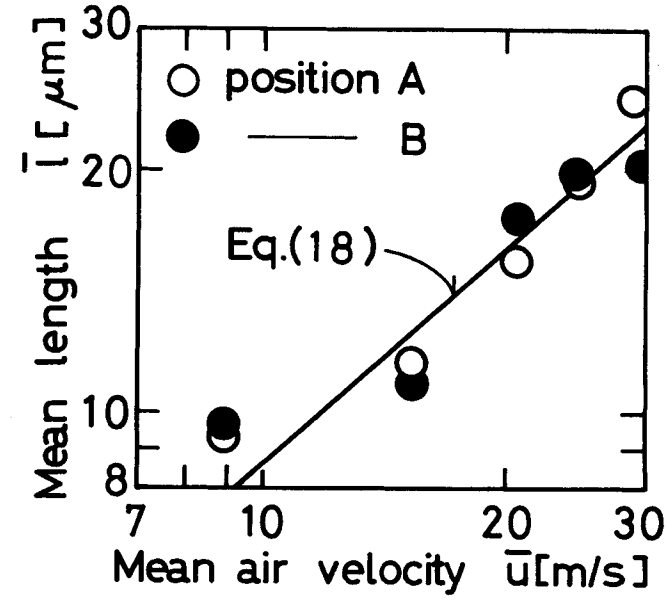

Fig. 7. Mean length of scars (quartz sand No. 8).

* It may be assumed that v_{ro} is proportional to $\bar{u}$ (Vollheim, 1971).

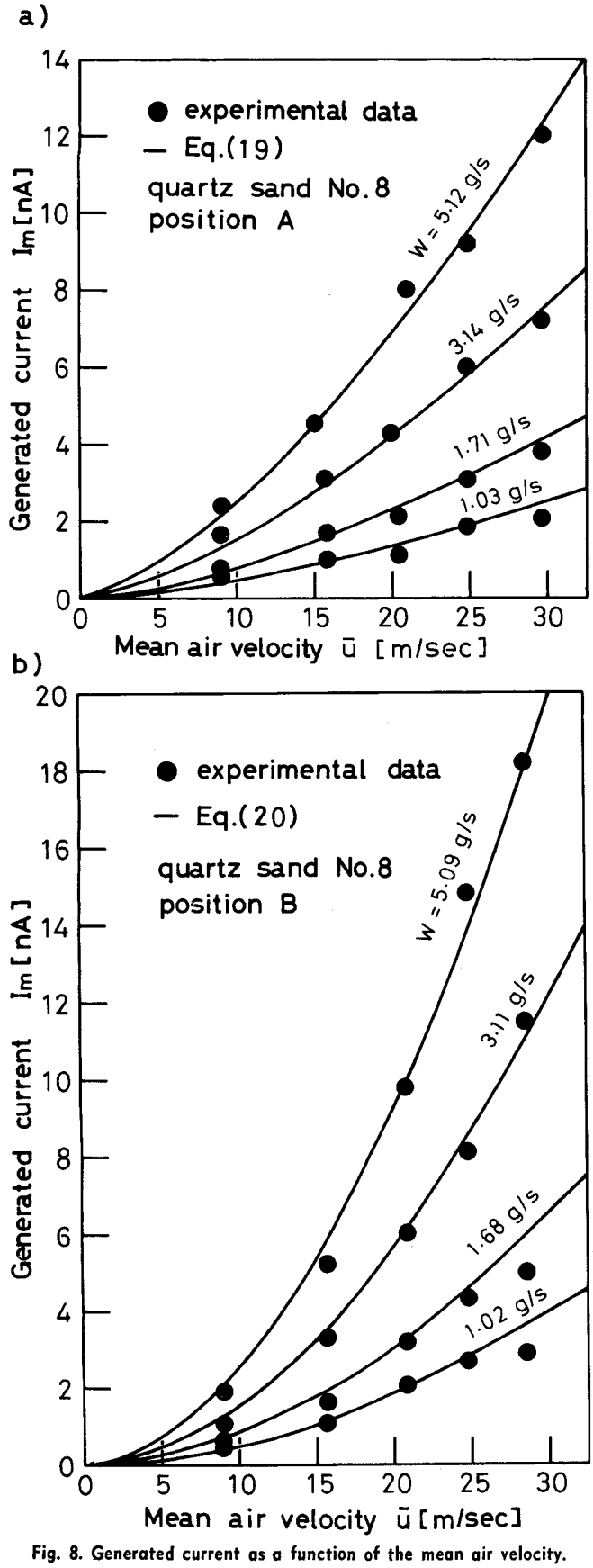

Fig. 8. Generated current as a function of the mean air velocity.

DURATION OF CONTACT

The experimentally obtained contact lengths are independent of the powder flow rate at constant air velocity. The experimental relation between the mean values $\bar{l}$ [μm] and air velocity $\bar{u}$ [m/s] is

$$\bar{l} = 1.1\,\bar{u}^{0.88} \tag{18}$$

This is shown by the solid line in Figure 7.

The mean length of the scars exceeds the corresponding width. This suggests sliding of the particle. Though the sliding velocity could not be measured in this experiment, it is assumed that the velocity is proportional to the mean air velocity $\bar{u}$. The duration of contact Δt is then proportional to $\bar{u}^{-0.12}$. This result may be qualitatively applicable to collision between particles and the metal wall as far as the contact is expected to be inelastic.

GENERATED ELECTRIC CURRENT

It was confirmed that the current generated was directly proportional to the powder flow rate. This relationship holds regardless of the position A, B, or C, and the powder used. However, the relation of current to mean air velocity depends on the position, as do the number of collisions shown in Figure 4. This suggests correspondence between the collision data and the currents generated.

If the experimental results on the number of collisions, area of contact, and duration of contact are substituted into Equation (6), the following equations are obtained for quartz sand No. 8:

$$|I_m| = 29\,K\,\bar{u}^{1.5}W \qquad \text{at position A} \tag{19}$$

$$|I_m| = 21\,K\,\bar{u}^{1.9}W \qquad \text{at position B} \tag{20}$$

where

$$K = \left| \frac{\epsilon_0 V_c \Delta x \pi D}{z_{0T}} \kappa\lambda \right| \tag{21}$$

κ and λ are dimensionless constants for the correction of area of contact and duration of contact, respectively. If the numerical K value is assumed to be 5.6×10^{-4} at position A and 3.2×10^{-4} at position B, the results calculated by Equations (19) and (20) are in good agreement with the experimental data on the electric current as shown in Figure 8. From the preceding theoretical development, the K values at A and B should be the same. The main cause of the error seems to be the differences in flow condition between the electric current experiment and the corresponding collision experiment. However, the power dependence supports the theoretical Equation (6) precisely because it is different at each test section.

The currents generated on the wall at positions B and C are proportional to the 1.7 to 1.9 power of the mean air velocity for all kinds of powders except morundum (aluminous abrasive which is an extraordinarily hard material). These results agree qualitatively with inelastic deformation theory. On the other hand, the data for morundum are proportional to the 1.3 to 1.5 power of the mean air velocity. This result agrees qualitatively with elastic deformation theory.

The experimental relationship between the current generated and the mean particle diameter was studied for eight quartz sands with diameters ranging from 14 to 330 μm and eight grades of morundum with diameters ranging from 50 to 760 μm. As the tests were repeated, the large particles became smaller so that the mean particle diameters gradually changed. Particle size distributions f were sometimes measured during the tests, and the mean particle diameters were calculated by the following equation (Masuda and Iinoya, 1972):

$$\bar{D}_p = 1 \Big/ \int_0^\infty (f/D_p)\, dD_p \tag{22}$$

Figure 9 shows the experimental relationship between the current generated per unit mass flow rate of powder, that is, the charge increment of powder per unit mass, and the mean particle diameter. The figure shows that the charge increment is inversely proportional to the mean particle diameter. Cole et al. (1969) show theoretically that the maximum possible charge on a particle q_∞ is proportional to D_p^2 to D_p^3, which means $(q/m_p)_\infty$ is proportional to D_p^{-1} to D_p^0. This relationship can also be shown by Equation (4). The second term of the denominator in Equation (4) is negligibly small for the experimental condition; hence $(q/m_p)_\infty$ is proportional to D_p^{-1}. If $n(\Delta x)/n_o$ in Equation (5) is independent of particle size, the current I_m is inversely proportional to mean particle diameter. To confirm this, further investigation of the number of collisions n will be undertaken. The experimental results on the current I_m can be expressed as

$$I_m = \gamma \frac{\bar{u}^\beta}{\bar{D}_p} W \qquad (23)$$

where the constants β and γ depend on the properties of the particles and of the pipe wall and position. Table 2 shows the constants determined by experiment at position B. At position C, the constant γ has about half the value listed in Table 2.

DISCUSSION

The experimental results support the contact electrification theory [Equation (6)]. The assumptions needed to establish the theory will now be discussed.

The first assumption is that the initial charge $|(q/m_p)_o|$ is much smaller than the maximum possible charge $|(q/m_p)_\infty|$. To confirm this, the charge on particles leaving the feeder was measured by means of a Faraday cage. It was found that the initial charge amounted, at the most, to that generated by flow through 15 to 30 cm of pipe, a distance considerably smaller than the total length of flow. This result justifies the first assumption.

The second assumption is that $n(x)$ and $n(\Delta x)$ are much smaller than n_o. To confirm this, the current $|I_m|$ generated on a test section of 15 cm length was measured at different flow lengths x from the inlet. The results, which were reported previously (Masuda et al., 1974), showed that current did not decrease with increasing x for the experimentally used flow lengths. Equation (2) shows that the current $|I_m|$ will decrease with x when the value of $n(x)$ is approximately equal to or greater than n_o. Since this decrease was not seen experimentally, the value of $n(x)$ must be considerably smaller than n_o. If $n(x)$ is much smaller than n_o, $n(\Delta x)$ must also be smaller.

The third assumption is that the relaxation time τ is much larger than the duration of contact Δt.

The value of τ was not measured experimentally, but an estimate of its magnitude can be based on the two alternative theories of the state of contact of a particle and the wall (Krupp, 1967; Sze, 1969).

Assuming there is a gap of a few Angstrom units between a particle and the wall (Krupp, 1967), the value of τ is larger than that estimated by assuming a contact transition region (Sze, 1969). Therefore, it is sufficient to estimate the value for the latter case.

Then, τ may be estimated from

$$\tau = RC = \rho\epsilon \qquad (24)$$

If a typical value of $5 \times \epsilon_o$ is assumed for ϵ, and specific resistance ρ is taken as $10^{13}\ \Omega$ cm, Equation (24) gives $\tau = 4.5$ s.

Since duration of contact Δt is approximately 10^{-6} s, the assumption $\tau >> \Delta t$ will hold for either theory.

While the transition region approach seems more realistic, further experiments are necessary to clarify this point.

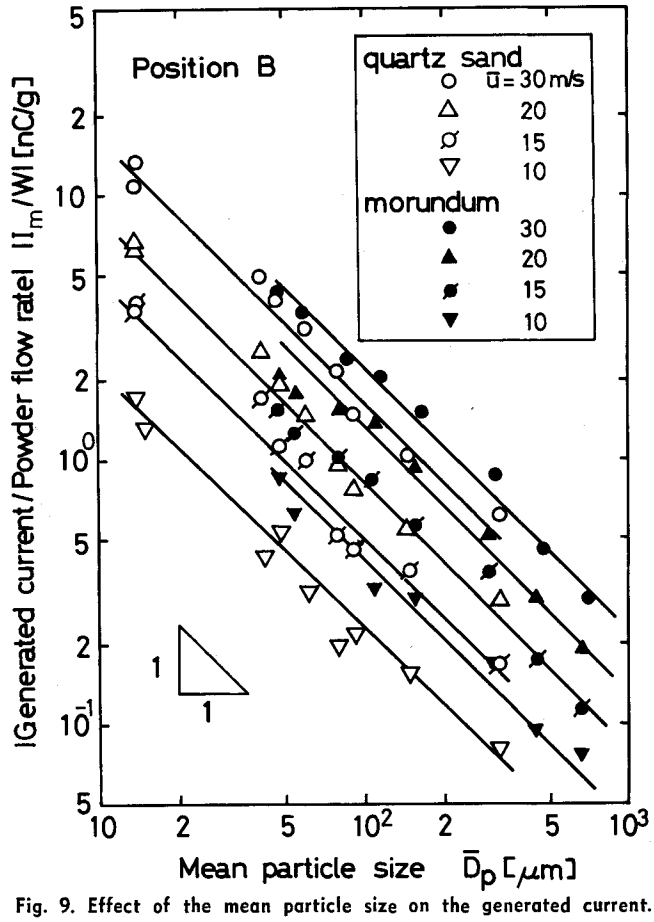

Fig. 9. Effect of the mean particle size on the generated current.

Table 2. Constants in Equation (23),* Vertical Position

Materials	γ	β
Quartz sand	+0.3	1.9
Vinyl chloride	−0.91	1.9
Morundum	−2.0	1.4
Flour	−2.5	1.9

* I_m [nA], $\bar{u}$[m/s], $\bar{D}_p$[μm], W[g/s].

NOTATION

b = width of scar
C = electric capacitance
D = inside diameter of pipe
D_p = particle diameter
d = depth of deformed region
e = coefficient of restitution
E = Young's modulus
f = frequency distribution of particle size (μm^{-1})
F_R = normal component of the impulse by particle motion
I_m = current generated on an insulated section of length Δx
K = constant defined by Equation (21)
l = length of scar
m = solids-air mass flow ratio $\left(= W/\frac{\pi}{4} D^2 \rho_a \bar{u}\right)$
m_p = mass of a particle
M = rate of increase of the number of collisions per unit area in the steady state = dN/dt
N = number of collisions per unit area

$n(x)$ = number of collisions of a particle
$n(\Delta x)$ = number of collisions of a particle between x and $x + \Delta x$
n_o = relaxation number of collisions when $n(x) = n_o$, $q/m_p = 0.632\ \{(q/m_p)_\infty - (q/m_p)_o\}$
P = constant yield pressure
q = charge on a particle
$(q/m_p)_o$ = initial charge per unit mass of particles at $x = o$
$(q/m_p)_\infty$ = maximum possible charge per unit mass of particles at $x = \infty$
R = internal resistance
S = area of contact
Δt = duration of contact
ΔT = time required for deformation
u = air velocity
u^* = friction velocity
v = axial component of particle velocity
v_r = radial component of particle velocity
v_{ro} = radial component of particle velocity just before impact
V = deformed volume
V_c = contact potential difference
W = powder mass flow rate
W_R = work done by normal impulse
x = flow length from inlet ($x = o$)
z_o = gap between contact bodies

Greek Letters

β = constant in Equation (23)
γ = constant in Equation (23)
ϵ = dielectric constant of a particle
ϵ_o = dielectric constant of air, 8.85×10^{-12} F/m
κ = constant in Equation (21)
λ = constant in Equation (21)
μ = viscosity of air
ρ = specific resistance of particle
ρ_a = density of air
ρ_p = density of particle
τ = relaxation time ($= RC$)

Superscript

— = mean value

LITERATURE CITED

Cole, B. N., M. R. Baum, and F. R. Mobbs, "An Investigation of Electrostatic Charging Effects in High-speed Gas-solids pipe Flows," *Proc. Inst. Mech. Engrs.*, **184**, 3C77 (1969-70).

Krupp, H., "Particle Adhesion Theory and Experiment," *Advan. Colloid Interface Sci.*, **1**, 111 (1967).

Masuda, H., and K. Iinoya, "Mean Particle Diameter in an Analysis of a Particulate Process," *Mem. Faculty Eng. Kyoto Univ.*, **34**, 344 (1972).

Masuda, H., T. Komatsu, M. Hirose, and K. Iinoya, "Static Electrification in Gas-solids Pipe Flow," Preprints of the 39th Annual Meeting of the Soc. of Chem. Engrs., Japan (in Japanese) p. 170 (1974).

Powell, F., and B. W. Quince, "The Kinetics of Impact in Drop-weight Experiments," *J. Phys. D.; Appl. Phys.*, **5**, 1540 (1972).

Shaw, D. F., *An Introduction to Electronics*, p. 245, Longmans, London, England (1962).

Ström, L., "Transmission Efficiency of Aerosol Sampling Lines," *Atmos. Env.*, **6**, 133 (1972).

Sze, S. M., *Physics of Semiconductor Devices*, p. 90, Wiley, New York (1969).

Timoshenko, S., Strength of Materials, Van Norand, New York (1930).

Vick, F. A., "Theory of Contact Electrification," *Brit. J. Appl. Phys.*, **4**, S1 (1953).

Vollheim, R., *Pneumatischer Transport*, p. 35, VEB, Leipzig (1971).

Manuscript received July 8, 1975; revision received January 20, and accepted February 26, 1976.

The Steady and Unsteady State Analysis of a Simple Gas Centrifuge

The operating theory of the gas centrifuge is developed under both steady and unsteady state behavior. It is shown that countercurrent flow patterns in a gas centrifuge enhance the possible separation. The effect of self-diffusion of the gaseous mixtures is shown to be significant with low molecular weight gases but of less significance with heavy gases such as uranium isotopes. The time required to develop steady state pressure and concentration profiles is in the order of minutes, even with no net flow to and from the machine.

STEVEN R. AUVIL

and

BRUCE W. WILKINSON

Department of Chemical Engineering
Michigan State University
East Lansing, Michigan 48824

SCOPE

The gas centrifuge as a processing tool has not been widely studied. Its principal application to date has been in the field of isotope separation. The elementary theory of various gas centrifuge types has been reported in the literature to the point where a countercurrent centrifuge appears to be the most useful type. The analysis of flow patterns within such a separator and the evaluation of the optimal magnitude of flows has not been reported. Furthermore, the times required to achieve a fully developed flow pattern have not been considered, even though the flow characteristics and transient times become very important in the design of a gas centrifuge. These factors play an important part in the potential application of the gas centrifuge to the processing of low molecular gases, where the self-diffusion is large.

Correspondence concerning this paper should be addressed to Bruce W. Wilkinson. Steven R. Auvil is with Monsanto Company, St. Louis, Missouri.